

## Intercontinental Transport and Chemical Transformation 2002 (ITCT 2K2) and Pacific Exploration of Asian Continental Emission (PEACE) experiments: An overview of the 2002 winter and spring intensives

D. D. Parrish,<sup>1</sup> Y. Kondo,<sup>2</sup> O. R. Cooper,<sup>1,3</sup> C. A. Brock,<sup>1,3</sup> D. A. Jaffe,<sup>4</sup> M. Trainer,<sup>1</sup> T. Ogawa,<sup>5</sup> G. Hübler,<sup>1</sup> and F. C. Fehsenfeld<sup>1</sup>

Received 3 May 2004; accepted 17 September 2004; published 12 November 2004.

[1] In the winter and spring of 2002, airborne and ground-based measurements of O<sub>3</sub>, aerosols, and their precursors were made in the eastern and western North Pacific regions. Three field studies were conducted by an international team of scientists collaborating as part of the Intercontinental Transport and Chemical Transformation (ITCT) program, an activity of the International Global Atmospheric Chemistry (IGAC) project of the International Geosphere-Biosphere Program (IGBP). Previous measurements have indicated that the transport of Asian emissions across the North Pacific Ocean influences the concentrations of trace tropospheric species over the Pacific and even the west coast of North America. In this special section, the recently acquired data are used to better characterize the contribution of continental sources to the aerosol, ozone, and related trace species concentrations over the North Pacific. This overview is aimed at providing the operational and logistical context of the study and introducing the principal findings and conclusions that have been drawn from the results.

*INDEX TERMS:* 0365 Atmospheric Composition and Structure: Troposphere—composition and chemistry; 0368 Atmospheric Composition and Structure: Troposphere—constituent transport and chemistry; 0322 Atmospheric Composition and Structure: Constituent sources and sinks; *KEYWORDS:* intercontinental transport, long-range transport, ozone, aerosols, ITCT 2K2, PEACE B

**Citation:** Parrish, D. D., Y. Kondo, O. R. Cooper, C. A. Brock, D. A. Jaffe, M. Trainer, T. Ogawa, G. Hübler, and F. C. Fehsenfeld (2004), Intercontinental Transport and Chemical Transformation 2002 (ITCT 2K2) and Pacific Exploration of Asian Continental Emission (PEACE) experiments: An overview of the 2002 winter and spring intensives, *J. Geophys. Res.*, 109, D23S01, doi:10.1029/2004JD004980.

### 1. Introduction

[2] Over the past two decades there have been increasing indications that chemical pollutants, even compounds with reasonably short lifetimes, can be detected at great distances from their sources. To implement a systematic study of the intercontinental transport of anthropogenic emissions, their influence on the photochemistry of remote regions, and their possible impact on the air quality of downwind continents, a coordinated international research program was organized within the framework of the International Global Atmospheric Chemistry Project (IGAC): the Intercontinental Transport and Chemical Transformation (ITCT). The first

field programs carried out as part of ITCT were the Pacific Exploration of Asian Continental Emission (PEACE)-A and PEACE-B campaigns and the ITCT 2K2 campaign. PEACE-A was conducted in January 2004, and PEACE-B and ITCT 2K2 were conducted in coordination in April–May 2004. Both PEACE campaigns used the Gulf-stream II (G-II) aircraft, chartered by Japan Aerospace Exploration Agency (JAXA) flying from Nagoya (35°N, 137°E) and Kagoshima (32°N, 131°E), Japan. The ITCT 2K2 campaign used the NOAA WP-3D aircraft flying from Monterey, California (36.6°N, 122°W), and instrumented a ground site at Trinidad Head, California where the NASA Advanced Global Atmospheric Gases (AGAGE) program maintains a baseline station and regularly launches O<sub>3</sub> sondes. Also operating in close coordination, the Photochemical Ozone Budget of the Eastern North Pacific Atmosphere (PHOBEA) 2002 measured from a small research aircraft over the eastern North Pacific and the Cheeka Peak, Washington, surface site.

[3] The study of tropospheric photochemistry over the North Pacific has been initiated over the past two decades, although earlier studies documented the long-range transport of dust from Asia [Prospero, 1979; Duce *et al.*, 1980]. The springtime is of particular interest since it is the season

<sup>1</sup>Aeronomy Laboratory, National Oceanic and Atmospheric Administration, Boulder, Colorado, USA.

<sup>2</sup>Research Center for Advanced Science and Technology, University of Tokyo, Tokyo, Japan.

<sup>3</sup>Also at Cooperative Institute for Research in Environmental Sciences, University of Colorado, Boulder, Colorado, USA.

<sup>4</sup>Interdisciplinary Arts and Sciences, University of Washington-Bothell, Washington, USA.

<sup>5</sup>Earth Observation Research and Application Center, Japan Aerospace Exploration Agency, Tokyo, Japan.

with the strongest outflow of Asian emissions to the Pacific, and also has the most extensive observational database. In this season in the source outflow region the NASA Global Tropospheric Experiment (GTE) missions 1994 PEM-West B [Hoell *et al.*, 1997] and 2001 Transport and Chemical Evolution Experiment over the Pacific (TRACE-P) [Jacob *et al.*, 2003] focused on oxidant photochemistry. The 2001 fourth Aerosol Characterization Experiment (ACE-Asia) [Huebert *et al.*, 2003] quantified the spatial and vertical distribution of aerosol properties in this same region. The Mauna Loa Observatory Photochemistry Experiment (MLOPEX) was conducted in the central subtropical Pacific during May and June 1988 [Ridley and Robinson, 1992] and during four one-month-long intensive periods in each season of 1991/1992 [Atlas and Ridley, 1996] in the central North Pacific on Hawaii. Hess [2001] analyzed the spring-time MLOPEX results with respect to the transport and photochemical processing of the measured species.

[4] Studies over the eastern North Pacific have been more limited. The NASA GTE program conducted part of the Chemical Instrumentation and Evaluation (CITE) 1C Study over the western United States and the adjoining Pacific Ocean [Hoell *et al.*, 1990]. Andreae *et al.* [1988] found that sulfur dioxide and sulfate in aerosols were largely associated with emissions of sulfur dioxide from sources located on the Asian continent. Parrish *et al.* [1992] found that levels of O<sub>3</sub>, peroxyacetyl nitrate (PAN), nitric acid (HNO<sub>3</sub>) and the light alkanes were enhanced during periods when trajectory analysis indicated rapid transport from Asia.

[5] More recently, the Photochemical Ozone Budget of the Eastern North Pacific Atmosphere (PHOBEA) surface and aircraft campaigns were conducted off the northwest coast of the United States in spring beginning in 1997. Surface observations made at the Cheeka Peak Observatory on the northwestern tip of Washington were used to quantify the in situ O<sub>3</sub> production [Jaffe *et al.*, 2001]. Airborne observations made in 1999 were used to derive the in situ O<sub>3</sub> production rates for the free troposphere in that region and the significance of PAN decomposition [Kotchenruther *et al.*, 2001]. In addition a number of episodes of transpacific long-range transport have been identified during these campaigns [Jaffe *et al.*, 2003a, and references cited therein]. Industrial pollutants and mineral dust were the primary species found in air masses that arrived over the northeastern Pacific via transpacific transport. The GEOS-CHEM model has modeled transpacific transport and confirmed that Asian industrial sources are a dominant source for CO and O<sub>3</sub> in the northeast Pacific region [Jaeglé *et al.*, 2003].

[6] The PEACE and ITCT 2K2 coordinated studies were organized around four major objectives: (1) to investigate the seasonal variation in the mode of horizontal and vertical transport and its effect on the distributions of ozone precursors and aerosols in the North Pacific troposphere, (2) to quantify seasonal variation of the oxidizing capacity and ozone budget over the western North Pacific from winter to late spring as a result of changes in key photochemical and transport processes, (3) to characterize the chemical composition of the air masses coming ashore at the U.S. West Coast, and to determine its relation to the sources and sinks of ozone and aerosols and (4) to explore the composition of these air masses as they are transported inland, and inves-

tigate the alteration in composition associated with the addition of emissions from U.S. West Coast sources.

[7] The ITCT 2K2 study was primarily an exploratory mission with additional specific science questions designed to guide mission planning: (1) Will measurements of trace chemicals or aerosol chemical composition provide elemental and/or chemical speciation fingerprints for different source classes or source regions? (2) What mechanisms control the export of emissions from Asia (and Mexico-Central America, and North America) to the North Pacific Ocean? (3) How does the composition of the anthropogenic emissions change during transport, and what is the effect upon ozone, aerosols and other photochemical products? (4) What are the magnitude and ultimate impact of emissions from commercial shipping and air transport in the Pacific? (5) Can we find evidence of influence from continental sources upwind of Asia (Europe, tropical regions, or globally circulated North American emissions)?

## 2. Design and Measurements

[8] PEACE-A was conducted in January 2004 and PEACE-B and ITCT 2K2 were conducted in coordination in April-May 2004. The timing of the PEACE missions, combined with the March 2001 TRACE-P study, provides coverage of the seasonal progression of O<sub>3</sub> photochemistry and O<sub>3</sub> precursor transport processes from winter to late spring [Kondo *et al.*, 2004]. We chose to focus on spring since it is the season with the strongest outflow of Asian emissions to the Pacific, has the most extensive past observational database, and encompasses the northern hemisphere tropospheric O<sub>3</sub> maximum that is thought to largely result from the maximum in the net photochemical production of O<sub>3</sub>.

[9] The major sampling regions over the North Pacific are shown in Figures 1 and 2. The PEACE program operated over the western North Pacific off the coast of Asia, both to the southeast and northwest of Japan in the Asian outflow region, while ITCT 2K2 focused upon the receptor region over the eastern North Pacific near the North American west coast.

### 2.1. Aircraft Instrument Payload and Flights

[10] In situ chemical data obtained on board the G-II aircraft were used for the PEACE study. The measured quantities included O<sub>3</sub>, CO, NMHCs, NO, total reactive nitrogen (NO<sub>y</sub>), H<sub>2</sub>O, and photolysis frequency of NO<sub>2</sub> ( $J(\text{NO}_2)$ ). The instruments used here are the same as those used for BIBLE-B campaigns [Kondo *et al.*, 2002], with an addition of an SO<sub>2</sub> instrument. Table 1 summarizes the techniques, uncertainties (accuracy and precision), and time resolutions of these measurements. Tables 2a and 2b summarize the flights for the winter and spring PEACE campaigns, and Figure 1 illustrates the flight tracks.

[11] The NOAA WP-3D Orion aircraft was instrumented for the ITCT 2K2 study with an ozone photochemistry payload that was augmented with measurements of aerosol composition. The aircraft could operate from the marine boundary layer (MBL) up to 8 km and had sufficient range to reach to the Canadian and the Mexican borders and well out into the North Pacific when stationed in Monterey, California. The payload used in previous studies measured

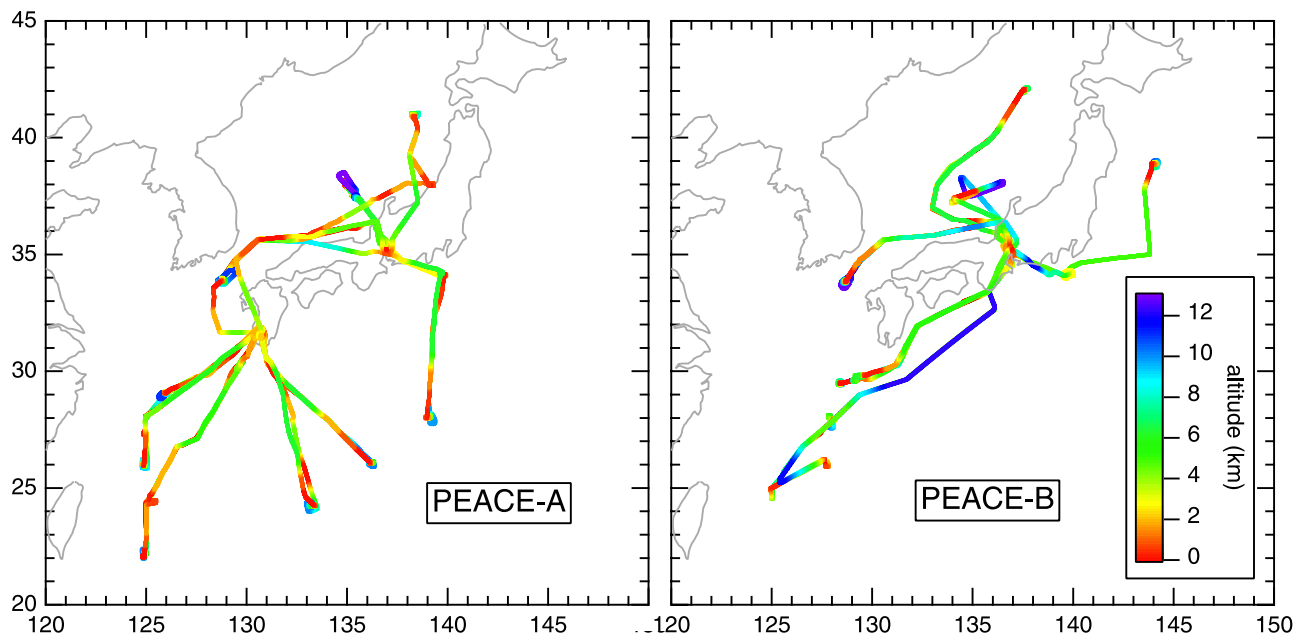


**Figure 1.** Maps indicating G-II aircraft flights during PEACE, color-coded according to altitude.

ozone, its precursors (volatile organic compounds and nitrogen oxides), products and by-products of the chemistry that produces ozone, size resolved aerosol number density, emission tracers ( $\text{SO}_2$ ,  $\text{CO}_2$ ,  $\text{CO}$  and certain VOCs), actinic fluxes, aircraft and meteorological state parameters. New aerosol instruments added for ITCT 2K2 included a single particle aerosol composition measurement provided by Particle Analysis by Laser Mass Spectrometry (PALMS) and the soluble bulk ionic composition measurements through particle into liquid sampling (PILS). A chemical ionization mass spectrometer measured  $\text{H}_2\text{SO}_4$  and OH radicals. Tables 3a and 3b summarize the WP-3D instrument characteristics. Table 4 and Figure 2 summarize the ITCT 2K2 flights.

## 2.2. Trinidad Head and PHOBEA Measurements

[12] The primary site instrumented for the ITCT 2K2 study operated at Trinidad Head, California ( $41^\circ 03' \text{N}$ ,  $124^\circ 09' \text{W}$ , 107 m asl) from 19 April to 22 May 2002. Volatile organic compounds were measured using a fully automated, in situ GC/MSD/FID system that is described in detail elsewhere [Millet *et al.*, 2004b].  $\text{O}_3$ ,  $\text{CO}$ ,  $\text{CO}_2$  and met parameters were measured [Goldstein *et al.*, 2004] along with  $\text{NO}$  and  $\text{NO}_x$ , and  $^{222}\text{Rn}$  using a dual-flow loop, two-filter radon detector [Whittlestone and Zahorowski, 1998]. Time-resolved aerosol measurements at the site included chemical composition using an Aerodyne aerosol mass spectrometer (AMS, Aerodyne Research Inc.) [Jimenez *et al.*, 2003; Allan *et al.*, 2003] and a particle-into-liquid sampler (PILS) [Weber *et al.*, 2001; Orsini *et al.*, 2003], number density (7 nm to 2.5  $\mu\text{m}$ ) using a condensation particle counter (CPC, model 3022a, TSI Inc.), and elemental composition using an 8-stage drum impactor and synchrotron X-ray fluorescence [Bench *et al.*, 2002; Cahill and Wakabayashi, 1993; Perry *et al.*, 1999]. Balloon-borne sondes launched daily from the site measured  $\text{O}_3$  concentrations and meteorological parameters with 1.2 second

resolution from the surface to approximately 35 km elevation. Direct, diffuse and total broadband solar irradiance (down welling), total down welling IR irradiance were also measured.

[13] In coordination with the ITCT 2K2 experiment, PHOBEA measurements of  $\text{CO}$ ,  $\text{O}_3$ , aerosol scattering (550 nm), elemental mercury, radon and meteorology parameters were made at the Cheeka Peak Observatory ( $48^\circ 18' \text{N}$ ,  $124^\circ 36' \text{W}$ , 480 m asl) from March through May 2002. The instrumental methods have been described previously [Jaffe *et al.*, 2001; Weiss-Penzias *et al.*, 2003]. From 29 March through 23 May 2002, 13 flights using a small

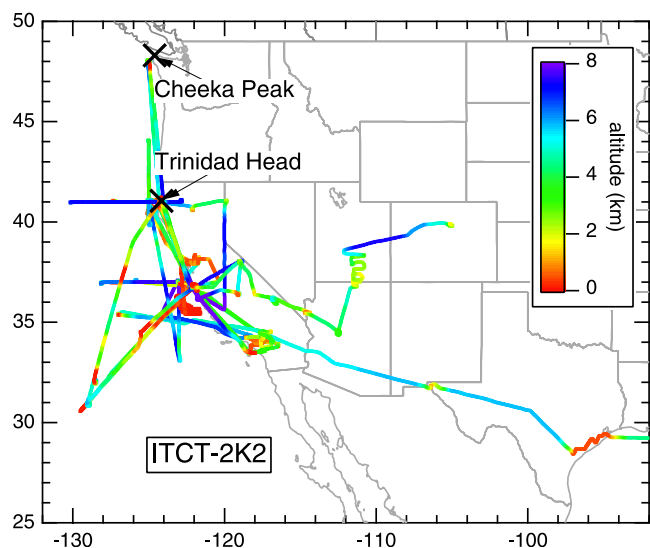


**Figure 2.** Map indicating WP-3D aircraft flights during ITCT 2K2, color-coded according to altitude. Note different altitude scale from Figure 1. The crosses indicate the two ITCT 2K2 surface sites.

**Table 1.** Instruments Used Aboard the GII Aircraft During PEACE-A and PEACE-B

Species/Parameter	Reference	Technique	Averaging Time	Accuracy	Precision	LOD <sup>a</sup>
NO	<i>Kondo et al.</i> [1997]	NO/O <sub>3</sub> chemiluminescence	1 s	8%	6 pptv	13 pptv
NO <sub>y</sub>	<i>Kondo et al.</i> [1997]	Au converter-chemiluminescence	1 s	17%	16 pptv	28 pptv
O <sub>3</sub>	<i>Kita et al.</i> [2002]	UV absorption	1 s	5%	0.6 ppbv	1.2 ppbv at 500 hPa
CO	<i>Takegawa et al.</i> [2001]	VUV resonance fluorescence	1 s	5%	1.4 ppbv	2.2 ppbv
CO <sub>2</sub>	<i>Machida et al.</i> [2002]	NDIR absorption	1 s	0.3 ppmv	0.1 ppmv	–
H <sub>2</sub> O		cryogenic chilled mirror hygrometer	60 s	±0.2°–0.5°C	±0.2°–0.5°C	–100°C to +20°C
H <sub>2</sub> O		thermoelectric hygrometer	60 s	±0.2°–1.0°C	±0.2°–1.0°C	–75°C to +50°C
NMHCs (C <sub>2</sub> –C <sub>10</sub> )	<i>Coleman et al.</i> [2001]	grab sample/GC	60 s	5–10%	1–3%	3 pptv
Halocarbons (C <sub>1</sub> –C <sub>2</sub> )	<i>Coleman et al.</i> [2001]	grab sample/GC	60 s	2–20%	1–10%	0.02–50 pptv
Alkyl nitrates (C <sub>1</sub> –C <sub>4</sub> )	<i>Coleman et al.</i> [2001]	grab sample/GC	60 s	10–20%	1–10%	0.02 pptv
Aerosol size distribution	<i>Liley et al.</i> [2002]	MASP	1 s	30%	<1%	0.1 cm <sup>–3</sup>
CN	<i>Liley et al.</i> [2002]	CN counter	1 s	5√N	0.04 cm <sup>–3</sup>	0.04 cm <sup>–3</sup>
Black carbon	<i>Liley et al.</i> [2002]	PSAP	10 s	40%	0.1 μg m <sup>–3</sup>	0.1 μg m <sup>–3</sup>
SO <sub>2</sub>		pulsed UV fluorescence	20 s	±0.4 ppbv	±0.2 ppbv	0.1 ppbv
J (NO <sub>2</sub> )	<i>Kita et al.</i> [2002]	filter radiometer	1 s	8%	1.5(–4) s <sup>–1</sup>	3.0(–4) s <sup>–1</sup>

<sup>a</sup>LOD, limit of detection.

research aircraft (Beechcraft Duchess 76) were conducted over the NE Pacific Ocean (47.8°–48.5°N and 123.9°–125.4°W, 0–6 km asl). On each flight, CO, O<sub>3</sub> and aerosol scattering (red, green and blue) were measured. *Bertschi et al.* [2004] describe the experimental methods, calibration procedures and other quality control measures for the PHOBEA airborne measurements.

### 2.3. Model Simulations

[14] The flight planning for the NOAA WP-3D was guided by forecasts from the CFORS-STEM, GEOS-CHEM, MOZART, and MATCH Eulerian chemical transport models (CTM), and the FLEXPART Lagrangian particle dispersion model. Most of the institutions that provided models also sent a scientist to the ITCT 2K2 operations center to interpret the model products and discuss the information with the flight coordinators.

[15] The NOAA Geophysical Fluid Dynamics Laboratory brought the MOZART-II CTM into the field. The model was run once per day in full chemistry mode using the forecast National Centers for Environmental Prediction

(NCEP) global AVN T170 wind fields (0.7° × 0.7° resolution). Products included fossil fuel, biomass burning and tagged regional CO tracers, as well as ozone, NO<sub>x</sub> and a stratospheric ozone tracer, all calculated at 1.9° × 1.9° resolution [*Horowitz et al.*, 2003].

[16] The University of Iowa ran the CFORS online tracer model based on forecast wind fields (200 km × 200 km resolution) from the RAMS model. Products included tagged regional CO tracers, and dust and sea salt tracers. Emissions from megacities were also tagged. In addition the STEM regional CTM was run once per day in full chemistry mode using the 60 × 60 km forecast wind fields of the RAMS model [*Tang et al.*, 2004].

[17] Harvard University and the University of Washington provided forecasts from the GEOS-CHEM global CTM [*Bey et al.*, 2001b], based on wind fields from the Goddard Earth Observing System (GEOS) of the NASA Global Modeling and Assimilation Office, regridded to 2° × 2.5° horizontal resolution. Products were provided once per day and included a total CO tracer using archived monthly OH fields [*Bey et al.*, 2001a] as well as Asian, European and

**Table 2a.** Dates and Locations of the PEACE-A GII Aircraft Flights at Nagoya (35°N, 137°E) and Kagoshima (32°N, 131°E)

Flight Number	Description	Date 2002	Day Number	Takeoff, UT	Landing, UT	Location (Latitude, Longitude)
1	Japan Sea (test flight)	6 Jan.	6	1127	1412	35°–39°N, 135°–137°E
2	Japan Sea (west of Japan)	7 Jan.	7	1146	1545	34°–36°N, 129°–137°E
3	Pacific Ocean (Miyakejima <sup>a</sup> )	10 Jan.	10	1017	1459	28°–35°N, 137°–140°E
4	Japan Sea (Nagoya–Niigata <sup>b</sup> )	11 Jan.	11	1020	1310	35°–38°N, 132°–139°E
5	Japan Sea (Niigata–Nagoya)	11 Jan.	11	1610	1825	35°–41°N, 137°–139°E
6	Japan Sea (Nagoya to Kagoshima)	13 Jan.	13	1111	1450	31°–36°N, 128°–136°E
7	East China Sea (southwest of Kushyu)	17 Jan.	17	1054	1440	27°–32°N, 128°–136°E
8	East China Sea (southwest of Kushyu)	18 Jan.	18	1104	1455	27°–32°N, 125°–131°E
9	East China Sea (Kagoshima–Miyakojima <sup>c</sup> )	19 Jan.	19	1002	1400	26°–32°N, 125°–131°E
10	East China Sea (Miyakojima–Kagoshima)	19 Jan.	19	1517	1720	22°–32°N, 125°–131°E
11	Pacific Ocean (southeast of Kushyu)	20 Jan.	20	1358	1740	25°–32°N, 125°–131°E
12	Pacific Ocean (south of Kushyu)	21 Jan.	21	1104	1516	26°–32°N, 131°–136°E
13	Japan Sea (Kagoshima to Nagoya)	23 Jan.	23	1105	1340	24°–32°N, 131°–134°E

<sup>a</sup>Miyakejima (34°N, 139°E).

<sup>b</sup>Niigata (39°N, 139°E).

<sup>c</sup>Miyakojima (25°N, 125°E).

**Table 2b.** Dates and Locations of the PEACE-B GII Aircraft Flights at Nagoya (35°N, 137°E)

Flight Number	Description	Date 2002	Day Number	Takeoff, UT	Landing, UT	Location (Latitude, Longitude)
1	Japan Sea (test flight)	21 April	111	1150	1450	35°–38°N, 134°–137°E
2	Japan Sea	23 April	113	0950	1430	35°–42°N, 133°–138°E
3	East China Sea (Nagoya-Naha <sup>a</sup> )	25 April	115	0950	1430	25°–35°N, 125°–137°E
4	East China Sea (Naha-Nagoya)	25 April	115	1545	1845	25°–35°N, 125°–137°E
5	East China Sea	27 April	117	1030	1515	25°–35°N, 125°–137°E
6	Japan Sea	29 April	119	1100	1515	34°–36°N, 128°–137°E
7	Japan Sea	8 May	128	1200	1605	34°–36°N, 129°–137°E
8	Pacific Ocean	11 May	131	0900	1340	34°–39°N, 137°–144°E
9	Pacific Ocean (Miyakejima)	14 May	134	0910	1130	34°–35°N, 137°–140°E
10	Japan Sea	14 May	134	1300	1710	34°–36°N, 128°–137°E
11	Japan Sea	15 May	135	1055	1600	34°–36°N, 128°–137°E
12	Pacific Ocean	16 May	136	1005	1425	30°–35°N, 129°–137°E

<sup>a</sup>Naha (26°N, 128°E).

North American fossil fuel tracers and a biomass-burning tracer. All products were updated twice daily.

[18] The Max-Planck-Institut für Chemie, in Mainz, Germany provided products from the MATCH-MPIC CTM over the internet [Lawrence *et al.*, 2003]. On the basis of the NCEP AVN wind fields, regridded to  $2.8^\circ \times 2.8^\circ$  resolution, the model produced 3-day forecasts of the global distributions of ozone and regional CO tracers. The tracer products were updated once per day.

[19] The FLEXPART Lagrangian particle dispersion model [Stohl *et al.*, 1998; Stohl and Thomson, 1999] provided 3-day forecasts of Asian, European and North American CO tracers. The tracer forecasts were updated 4 times per day, were driven by the  $1^\circ \times 1^\circ$  wind fields of the NCEP AVN model, and were made available at  $1^\circ \times 1^\circ$  resolution. The accuracy of the FLEXPART forecasts during the campaign is described by Forster *et al.* [2004].

[20] Finally, near-real-time geostationary satellite imagery were provided by the NOAA Aeronomy Laboratory. Data from the visible, infrared and water vapor channels of the

Japanese GMS-5 and the NOAA GOES-West satellites were downloaded hourly from UNIDATA and the University of Wisconsin. Panoramic views of the North Pacific basin were produced at 5 km resolution, and used to verify the transport pathways of the model tracers and to identify the weather systems advecting Asian pollution to the United States [Cooper *et al.*, 2004a, 2004b].

### 3. Overview of Results

#### 3.1. Studies in the Source Region: Overview of the Pacific Exploration of Asian Continental Emission (PEACE)-A and PEACE-B Campaigns

[21] Kondo *et al.* [2004] present box model calculations constrained by the observed concentrations of the O<sub>3</sub> precursors. These calculations show that the net O<sub>3</sub> formation in the boundary layer over the western North Pacific makes a major contribution to the column integrated net O<sub>3</sub> formation, especially in winter. The northwesterly wind in the boundary layer is highest over the western Pacific in

**Table 3a.** Instruments for Gas-Phase Measurements Aboard the WP-3D Aircraft During ITCT 2K2

Species/Parameter	Reference	Technique	Averaging Time	Accuracy	Precision	LOD
NO	Ryerson <i>et al.</i> [1999]	NO/O <sub>3</sub> chemiluminescence	1 s	5%	10 pptv	20 pptv
NO <sub>2</sub>	Ryerson <i>et al.</i> [2000]	photolysis-chemiluminescence	1 s	10%	30 pptv	100 pptv
NO <sub>y</sub>	Ryerson <i>et al.</i> [1999]	Au converter-chemiluminescence	1 s	10%	15 pptv	50 pptv
O <sub>3</sub>	Ryerson <i>et al.</i> [1998]	NO/O <sub>3</sub> chemiluminescence	1 s	2%	0.2 ppbv	0.2 ppbv
CO	Holloway <i>et al.</i> [2000]	VUV resonance fluorescence	1 s	2.5%	0.5 ppbv	1 ppbv
CO <sub>2</sub>	Parrish <i>et al.</i> [2004b]	NDIR absorption	1 s	0.3 ppmv	0.1 ppmv	–
H <sub>2</sub> O		Lyman alpha absorption	1 s	–	–	–
H <sub>2</sub> O		thermoelectric hygrometer	3 s	±0.2°–1.0°C	±0.2°–1.0°C	–75°C to +50°C
NMHCs (C <sub>2</sub> –C <sub>10</sub> )	Schauffler <i>et al.</i> [1999]	grab sample/GC	60 s	5–10%	1–3%	3 pptv
Halocarbons (C <sub>1</sub> –C <sub>2</sub> )	Schauffler <i>et al.</i> [1999]	grab sample/GC	60 s	2–20%	1–10%	0.02–50 pptv
Alkyl nitrates (C <sub>1</sub> –C <sub>5</sub> )	Schauffler <i>et al.</i> [1999]	grab sample/GC	60 s	10–20%	1–10%	0.02 pptv
VOCs	de Gouw <i>et al.</i> [2003]	proton transfer reaction mass spectrometer	15 s	10–20%	5–30%	50–250 pptv
PAN, PPN	Roberts <i>et al.</i> [2004]	dir. injection, GC/ECD	≈10 s	15%	2%	2 pptv
MPAN, PiBN, APAN	Roberts <i>et al.</i> [2004]	dir. injection, GC/ECD	≈10 s	20%	2%	3 pptv
HNO <sub>3</sub>	Neuman <i>et al.</i> [2002]	CIMS	1 s	15%	25 pptv	50 pptv
Hydroxyl radical		CIMS	2 m	?	?	$3 \times 10^5$ molecules cm <sup>-3</sup>
SO <sub>2</sub>	Ryerson <i>et al.</i> [1998]	pulsed UV fluorescence	3 s	10%	0.35 ppbv	1 ppbv
H <sub>2</sub> SO <sub>4</sub>	Eisele and Tanner [1993]	CIMS	1.1 s	35%	$1 \times 10^6$ molecules cm <sup>-3</sup>	$6 \times 10^6$ molecules cm <sup>-3</sup>

**Table 3b.** Instruments for Aerosol and Ancillary Data Measurements Aboard the WP-3D Aircraft During ITCT 2K2

Species/Parameter	Reference	Technique	Averaging Time	LOD
Aerosol single particle composition	<i>Thomson et al.</i> [2000]	particle analysis by laser mass spectrometer (PALMS)	single particle	<1 particles/cm <sup>3</sup>
Aerosol bulk ionic composition	<i>Weber et al.</i> [2001] and <i>Orsini et al.</i> [2003]	particle into liquid sampling (PILS)	3 m	<0.02 µg/m <sup>3</sup>
Small aerosol size distribution	<i>Brock et al.</i> [2000]	nucleation mode aerosol size spectrometer (NMASS)	1 s	0.005–0.06 µm
Large aerosol size distribution	<i>Brock et al.</i> [2003] and <i>Wilson et al.</i> [2004]	white light scattering (Clímet & LasAir) with low turbulence inlet	1 s	0.12–8.5 µm
Photolytic flux		280–400 nm spectrally resolved radiometer, zenith and nadir	1 s	unknown
Broadband radiation		Pyrgometer	1 s	3.5–50 µm
Broadband radiation		pyranometer	1 s	0.28–2.8 µm

winter because of the dominating Siberian high. It weakens with the progression of the season associated with the weakening of the Siberian high and strengthening of the Pacific high pressure. The net O<sub>3</sub> formation rate in the boundary layer is largest in winter because of the highest NO<sub>x</sub> concentrations, which are caused by efficient transport of NO<sub>x</sub> from the Asian continent due to high wind speeds and slow oxidation by OH. The net O<sub>3</sub> formation rate decreases from winter to spring because of the increase in the O<sub>3</sub> destruction rate associated with the increase in  $J(O^1D)$  and H<sub>2</sub>O. From January to April/May the column integrated O<sub>3</sub> formation rate is 6 times larger than the increase in the O<sub>3</sub> column of  $3.1 \times 10^{17}$  molecules cm<sup>-2</sup>, indicating that O<sub>3</sub> formed over the western Pacific is transported to regions over the Pacific outside the region of the present study.

[22] G. Chen et al. (A diagnostic analysis of winter/spring ozone budget based on ozonesonde and airborne observations from PEACE A/B and TRACE-P, submitted to *Journal of Geophysical Research*, 2004) (hereinafter referred to as Chen et al., submitted manuscript, 2004) present an analysis complementary to that of *Kondo et al.* [2004]. They construct an observation-based regional

tropospheric ozone column (TOC) budget in the western North Pacific for the time period from January to May. All budget terms, except for stratospheric flux estimates taken from current literature, are evaluated from either ozonesonde measurements recorded at Japanese stations (Naha, Kagoshima, and Tateno) or airborne data from PEACE-A, PEACE-B, and TRACE-P. Ozonesonde data show a significant winter/spring time increase of TOC, ranging, depending on latitude, from 16 to 48% of the average burden. The net effect of advective processes, estimated as a residual of the mass balance equation, is found to be a major sink of ozone to offset the photochemical production. The derived eastward advective flux is 20 times higher than the photochemical production. Thus the observed TOC trend is not controlled by local photochemistry. Because of this rapid advection, Chen et al. (submitted manuscript, 2004) conclude that the regional TOC seasonal variation is strongly modulated by the hemispheric ozone seasonal changes, while the net ozone exported from the western North Pacific is an important source for downwind regions where photochemistry is a net sink.

[23] *Takegawa et al.* [2004] estimate the removal rates of NO<sub>x</sub> and NO<sub>y</sub> in the boundary layer during the

**Table 4.** Dates and Locations of the ITCT 2K2 WP-3D Aircraft Flights

Flight Number	Description	Date 2002	Takeoff, UT	Landing, UT
1a	transit Tampa, Florida, to El Paso, Texas, sample Houston area chemical plants	22 April	1611	2157
1b	transit El Paso to Monterey, California	22 April	2305	0216
2	transect of cutoff low SSW of Monterey	25 April	1735	0108
3	step profile on west side of cutoff low	29 April	1715	2311
4	Trinidad Head flyby, ship plume study, Richmond/San Francisco Bay Area	2 May	1737	2325
5	intercept Asian outflow NW of Monterey	5 May	1831	0104
6	follow Asian outflow ashore	6 May	1818	0115
7	ship plume study, Richmond/San Francisco Bay Area, California Central Valley	8 May	1732	0028
8	vertical distribution along longitudinal transect over Trinidad Head	10 May	1807	0126
9	vertical distribution along latitudinal transect off U.S. West Coast	11 May	1811	0041
10	Los Angeles basin	13 May	1838	0140
11	Asian outflow in high-pressure system SW of Monterey	15 May	1813	0110
12	intercept Asian outflow SW of Monterey	17 May	1809	0144
13	transit Monterey, California, to Jefferson County, Colorado, sample Los Angeles outflow, power plant plume in SW Colorado, and forest fire plume	19 May	1813	0136

PEACE-A period. Correlations of CO with CO<sub>2</sub> and back trajectories are used to identify plumes strongly affected by Asian continental emissions.  $\Delta\text{CO}/\Delta\text{CO}_2$  ratios in the plumes generally fall within the variability range of the CO/CO<sub>2</sub> emission ratios derived from the emission inventory of *Streets et al.* [2003], demonstrating the consistency between the aircraft measurements and the emission characterization. The photochemical age of the plumes is derived from the observed  $\Delta\text{C}_2\text{H}_4/\Delta\text{C}_2\text{H}_2$  ratios and the OH concentration calculated by a constrained photochemical box model. The average lifetime of NO<sub>x</sub> in the plumes is estimated to be  $1.2 \pm 0.4$  days using the correlation with CO<sub>2</sub> and the plume age. It is shown that NO<sub>2</sub> + OH reaction and N<sub>2</sub>O<sub>5</sub> hydrolysis can likely account for most of the NO<sub>x</sub> loss processes under PEACE-A conditions. The average lifetime of NO<sub>y</sub> in the plumes is estimated to be  $1.7 \pm 0.5$  days, suggesting the importance of chemical processing near the source regions in determining the NO<sub>y</sub> budget.

[24] Transport processes that were responsible for export of anthropogenic emissions over the east Asia during the PEACE-B period are described by *Oshima et al.* [2004]. During this period a quasi-stationary frontal zone had formed over central China by low-level southerlies. Pronounced upward motion of air along the frontal zone followed by westerly transport by the subtropical jet over this system is found to be an efficient transport mechanism of pollutants emitted around central China. Episodic enhancements of convection play an important role producing the updrafts. Back trajectories of air parcels sampled onboard the aircraft show that 27% of air parcels sampled at altitudes above 4 km were likely influenced by convection over central China and other regions. These results are consistent with enhancements of CO and relatively high levels of Halon 1211 (a good tracer of Chinese anthropogenic emissions) observed at altitudes between 5 and 10 km during several flights.

[25] Measurements of O<sub>3</sub> by ozonesondes were made over subtropical and midlatitude China during the PEACE-A period [*Chan et al.*, 2004]. The O<sub>3</sub> concentrations in the boundary layer were similar to those observed over the western Pacific, except near Beijing, where titration by NO reduced O<sub>3</sub>. Influx of O<sub>3</sub> from the stratosphere likely caused occasional increases in O<sub>3</sub> in the free troposphere.

### 3.2. Overviews of Transport and Photochemistry

[26] Six analyses describe the transport pathways from Asia to North America, two of which also model the photochemistry during transit. *Forster et al.* [2004] used the FLEXPART particle dispersion model to estimate the quantity of Asian CO transported across the western edge of North America. On the basis of a 15-year climatology, CO transport has a springtime maximum and summer minimum, with the springtime flux centered at 35°N and 8 km altitude. During the ITCT period the CO flux was 8% less than the climatological mean for April and May.

[27] *Liang et al.* [2004] simulated global CO transport for the March 2001 through May 2002 time period with the GEOS-CHEM CTM and identified one winter and four spring cases when Asian transport events increased CO at

Cheeka Peak Observatory by 20–40 ppbv. Most events reaching the eastern North Pacific lower troposphere were the result of boundary layer outflow behind cold fronts (for spring) or ahead of cold fronts (for other seasons) followed by low-level transpacific transport. In contrast, lifting ahead of cold fronts on the western side of the Pacific was associated with 78% of the events reaching the eastern North Pacific middle and upper troposphere.

[28] *Cooper et al.* [2004a, 2004b] provide detailed case studies of transpacific warm conveyor belt (WCB) transport. The first analysis [*Cooper et al.*, 2004b] showed that a WCB that formed over Japan entrained air from a variety of source regions including the marine boundary layer, the polluted lower troposphere of east Asia, the midtroposphere and an aged upwind WCB. The polluted WCB had decayed by the time it reached the U.S. West Coast and advected across the country with only minimal impact on the lower troposphere. The second study [*Cooper et al.*, 2004a] described the manner in which stratospheric intrusions decay and disperse into the remnants of polluted WCBs above the Pacific, blurring the chemical distinction between anthropogenic and stratospheric influenced air masses.

[29] *Hudman et al.* [2004] used the global GEOS-CHEM CTM in full chemistry mode [*Bey et al.*, 2001b] to interpret the ITCT 2K2 and PEACE-B aircraft observations, and to assess the impact of Asian emissions on U.S. surface ozone. They argue that PAN decomposition represents a major and possibly dominant component of the ozone enhancement in transpacific plumes carrying Asian emissions. They also found that strong dilution of Asian pollution plumes takes place during entrainment in the U.S. boundary layer, greatly reducing their impact at U.S. surface sites.

[30] *Tang et al.* [2004] modeled the photochemistry of the eastern North Pacific and U.S. West Coast using the STEM-2K3 regional CTM. Focusing on two flights they found the ozone net chemical budgets were negative in regions dominated by Asian influences and positive in polluted American air masses. The results also indicated that the low NO<sub>y</sub> levels in Asian air masses was partly due to the conversion of gaseous HNO<sub>3</sub> to nitrate particle. Surface pollution episodes at Trinidad Head were the result of calm conditions that allowed the accumulation of local emissions.

### 3.3. Studies in the Receptor Region: PHOBEA Results

[31] The PHOBEA spring 2002 airborne data reveal numerous episodes of long-range transport (LRT) of pollutants from the Eurasian continent [*Bertschi et al.*, 2004]. A substantial episode on 15 April 2002 was associated with LRT from industrial sources in Asia, similar in many respects to previous LRT episodes [*Jaffe et al.*, 2003a; *Price et al.*, 2003], in that it contained significant enhancements of CO, O<sub>3</sub> and aerosols. However since the measurements continued later in the spring than in previous years, *Bertschi et al.* [2004] observed evidence of LRT of biomass burning sources in Siberia. These plumes were transported to North America in 6–8 days. Confirmation of the biomass burning source for several LRT events in May was made by using satellite imagery, back trajectories, the GEOS-CHEM global chemical transport model, and the chemical signature of the observed plumes (e.g., CO to aerosol ratio).

[32] *Price et al.* [2004] describe the dilution and photochemistry during 11 transpacific LRT episodes from our observations taken between 1997 and 2002. This work identifies two key processes that help explain variations in  $O_3$  mixing ratios during LRT events: presence of mineral dust and transport in the boundary layer. For those LRT events with significant boundary layer transport or with large amounts of mineral dust, relatively low ozone enhancements were seen. Only when the air mass was transported in the free troposphere and in the absence of large amounts of mineral dust is an  $O_3$  enhancement identified.

[33] The GEOS-CHEM model was used both for forecasting LRT and in postmission analysis [*Liang et al.*, 2004; *Goldstein et al.*, 2004; *Weiss-Penzias et al.*, 2004]. *Liang et al.* [2004] quantified the Asian influence on CO mixing ratios in the eastern North Pacific atmosphere over a full seasonal cycle, including the ITCT 2K2 time period. They found that Asian sources were responsible for 24–30% of the CO in this region. *Liang et al.* [2004] also carried out a systematic analysis of the meteorological mechanisms leading to transpacific transport events. Frontal lifting and zonal transport in the free troposphere was the dominant mechanism to bring pollutants to the middle and upper troposphere over the eastern North Pacific. The majority of events reaching CPO below 2 km altitude were the result of boundary layer export either behind or ahead of midlatitude cyclones, followed by low-level transport across the Pacific. *Weiss-Penzias et al.* [2004] interpret a full year of observations from CPO using both the GEOS-CHEM model and back trajectories.

### 3.4. Gas-Phase Composition and Photochemistry

#### 3.4.1. Gas-Phase Species in the Marine Boundary Layer

[34] *Millet et al.* [2004a] characterize the composition of the volatile organic compounds (VOCs) in the eastern North Pacific marine boundary layer, and use the observed variability of the concentrations to infer many aspects of transport and transformation of species in the sampled air masses. They report hourly in situ measurements of  $C_1$ – $C_8$  speciated VOCs obtained at Trinidad Head, California, in April and May 2002. They utilize factor analysis to elucidate the dominant processes affecting the concentrations, and to characterize the sources of the measured species. Strong decreases in background concentrations were observed for several of the VOCs during the experiment due to seasonal changes in OH concentration. CO is the most important contributor to the total measured OH reactivity at the site at all times. Oxygenated VOCs are the primary component of both the total VOC burden and of the VOC OH reactivity. VOC variability exhibited a strong dependence on residence time ( $s_{\ln X} = 1.55 \times \tau^{-0.43}$ ,  $r^2 = 0.98$ ; where  $s_{\ln X}$  is the standard deviation of the natural logarithm of the mixing ratio), and this relationship is used, in conjunction with measurements of  $^{222}\text{Rn}$ , to estimate the average OH concentration during the study period ( $6.1 \times 10^5$  molecules  $\text{cm}^{-3}$ ). They also employ the variability-lifetime relationship defined by the VOC data set to estimate submicron aerosol residence times as a function of chemical composition. Two independent measures of aerosol chemical composition yield consistent residence

time estimates, 3–7 days for aerosol nitrate, organics, sulfate, ammonium, and sea salt. The lifetime estimate for methane sulfonic acid ( $\sim 12$  days) is slightly outside of this range, and the lifetime of the total aerosol number density is estimated at 9.8 days.

[35] *Goldstein et al.* [2004] measured a wide suite of trace gases and aerosols in concert with the VOC measurements of *Millet et al.* [2004a]. They use a combination of in situ ground-based measurements from Trinidad Head, California, chemical transport modeling, and backward trajectory analysis to examine the impact of long-range transport from Asia on the composition of air masses arriving at the California coast at the surface. The impact of Asian emissions is explored in terms of both episodic enhancements and contribution to background concentrations. The variability in CO concentrations was largely driven by North American emissions, and episodic enhancements due to Asian plumes were not observable. Nevertheless, model simulations suggest that Asian emissions were responsible for 33% of the measured CO, a larger mean contribution than direct emissions from any other region of the globe. Surface ozone levels are found to depend primarily on local atmospheric mixing, with surface deposition leading to low concentrations under stagnant conditions. Model simulations suggest that on average  $4.5 \pm 1.1$  ppb of ozone (11% of average observed) was transported from Asia.

[36] The study by *de Gouw et al.* [2004] used the measurements of acetonitrile ( $\text{CH}_3\text{CN}$ ) from the NOAA WP-3D aircraft to demonstrate the utility of that species as a biomass-burning tracer. Acetonitrile was strongly enhanced in the plumes from two forest fires, confirming its presence in biomass burning emissions. The emission ratios of acetonitrile relative to CO in the two plumes were slightly higher than previously reported values for fires burning in other fuel types. No significant acetonitrile release was observed in the Los Angeles basin or from other point sources (ships and a power plant). Acetonitrile concentrations were significantly reduced in the marine boundary layer indicating the presence of an ocean uptake sink. Increased loss of acetonitrile was observed close to the coast, suggesting that acetonitrile was efficiently lost by dissolving in the upwelling ocean water, or by biological processes in the surface water.

#### 3.4.2. Trends in Marine Boundary Layer Photochemistry

[37] Partially on the basis of data collected during ITCT 2K2, *Jaffe et al.* [2003b] conclude that  $O_3$  in air arriving at the North American coast from the eastern Pacific in spring has increased by approximately 10 ppbv, i.e., 30% from the mid-1980s to the present. *Parrish et al.* [2004a] provide substantial evidence that the increased  $O_3$  has resulted from a marked change in the photochemical environment in the springtime troposphere of the North Pacific. They note (1) larger increases in the minimum observed ozone levels and much more modest increases in the maximum levels, (2) increasing PAN levels that parallel trends in  $\text{NO}_x$  emissions, and (3) decreasing efficiency of photochemical  $O_3$  destruction (less negative  $P(\text{O}_3)$ ). This changing photochemical environment is hypothesized to be due to increasing anthropogenic emissions from Asia, which are believed to have increased substantially over the 2 decades preceding

the study. The influence of the increased emissions is proposed to have changed the spring time Pacific tropospheric photochemistry from predominately ozone destroying to more nearly ozone producing. However, chemical transport model calculations indicate the possible influence of a confounding factor; unusual transport of tropical air to the western North Pacific may have played a role in this apparent trend in the photochemistry.

### 3.4.3. Gas-Phase Species in the Eastern North Pacific Midtroposphere

[38] Nowak *et al.* [2004] investigate the gas-phase chemical characteristics of emission plumes transported from Asia across the Pacific Ocean. Plumes measured from an aircraft are separated from background air by using 1-s measurements of carbon monoxide (CO), total reactive nitrogen ( $\text{NO}_y$ ) and other gas-phase species along with back trajectory analysis. Asian transport plumes with CO mixing ratios greater than 150 ppbv are identified on seven flights. Correlations between CO and  $\text{O}_3$  and  $\text{NO}_y$  are used to characterize the plumes. The  $\text{NO}_y/\text{CO}$  ratios were similar in each plume, but significantly lower than those derived from Asian emission inventories. Despite the similar  $\text{NO}_y/\text{CO}$  ratios the three strongest transport plumes exhibited differing  $\text{NO}_y$  partitioning. PAN dominated  $\text{NO}_y$  in the two plumes that were transported in cold, high-latitude and high-altitude regions, whereas  $\text{HNO}_3$  dominated in the one plume transported in warmer, lower latitude and altitude regions. Additional gas-phase species enhanced in one or more of these plumes include sulfuric acid, methanol, acetone, propane, and ethane. The  $\text{O}_3/\text{CO}$  ratio varied among the plumes and was affected by the mixing of anthropogenic and stratospheric influences. The complexity of this mixing prevents the determination of the relative contribution of anthropogenic and stratospheric influences to the observed  $\text{O}_3$  levels.

[39] During research flights on 5 and 17 May, strong enhancements of carbon monoxide (CO) and other species were observed in air masses that had been transported from Asia [de Gouw *et al.*, 2004]. The hydrocarbon composition of the air masses indicated that the highest CO levels were related to fossil fuel use. During the flights on 5 and 17 May and other days, the levels of several biomass-burning indicators increased with altitude. This was true for acetonitrile ( $\text{CH}_3\text{CN}$ ), methyl chloride ( $\text{CH}_3\text{Cl}$ ), the ratio of acetylene ( $\text{C}_2\text{H}_2$ ) to propane ( $\text{C}_3\text{H}_8$ ), and, on 5 May, the percentage of particles measured by the PALMS (particle analysis by laser mass spectrometry) instrument that were attributed to biomass burning on the basis of their carbon and potassium content. An ensemble of back-trajectories, calculated from the U.S. West Coast over a range of latitudes and altitudes for the entire ITCT 2K2 period, showed that air masses from Southeast Asia and China were generally observed at higher altitudes than air from Japan and Korea. Emission inventories estimate the contribution of biomass burning to the total emissions to be low for Japan and Korea, higher for China, and the highest for Southeast Asia. Combined with the origin of the air masses versus altitude, this qualitatively explains the increase with altitude, averaged over the whole ITCT 2K2 period, of the different biomass burning indicators.

[40] Measurements of PANs, peroxyacetic nitric anhydride ( $\text{CH}_3\text{C}(\text{O})\text{OONO}_2$ ; PAN), and peroxypropionic nitric anhydride ( $\text{CH}_3\text{CH}_2\text{C}(\text{O})\text{OONO}_2$ ; PPN) were made in the spring of 2002, off the west coast of North America, as part of the Intercontinental Transport and Chemical Transformation project [Roberts *et al.*, 2004]. Long-range transport events from Asia were observed in which PAN and PPN were as high as 650 pptv and 90 pptv respectively. Moreover, these two species constituted as much as 80% of the odd-nitrogen ( $\text{NO}_y$ ) in those air masses, and median PAN/ $\text{NO}_y$  was more than 60% at altitudes of 4 km and above. Mixing ratios of PAN and PPN were also elevated in the marine boundary layer (MBL) close to the west coast of California, probably as a result of maritime  $\text{NO}_x$  emissions, which provide the raw materials to photochemically produce PANs.

[41] A ship plume experiment was carried out about 100 km off the California coast during the recent NOAA airborne field campaign ITCT 2K2 (G. Chen, An investigation of the chemistry of ship emission plumes during ITCT 2002, submitted to *Journal of Geophysical Research*, 2004). Observations demonstrate a very short  $\text{NO}_x$  lifetime ( $\sim 1.8$  hours) inside the ship plume compared to  $\sim 6.3$  hours in the background marine boundary layer. An analysis with a photochemical model suggests that more than 80% of the  $\text{NO}_x$  loss was due to the  $\text{NO}_2 + \text{OH}$  reaction; the remainder was by PAN formation, which can be considered as a  $\text{NO}_x$  reservoir species for the conditions encountered. The model underestimated in-plume  $\text{NO}_x$  loss rate by about 30%. A comparison of measured to predicted  $\text{H}_2\text{SO}_4$  in the plumes suggests the model may underestimate OH by as much as a factor of 2. However, model simulation of in-plume  $\text{O}_3$  production agrees well with the observations, suggesting that model predicted peroxy radical ( $\text{HO}_2 + \text{RO}_2$ ) levels are reasonable. The largest model bias was seen in the comparison of  $\text{HNO}_3$ . The model overestimated in-plume  $\text{HNO}_3$  by about a factor of 6. This is most likely caused by underestimated  $\text{HNO}_3$  sinks, such as particle scavenging of  $\text{HNO}_3$ . However, available data did not allow a conclusive test of this possible loss process. Future studies should revisit these issues to further test our understanding of the ship plume chemical processes.

### 3.5. Aerosols in the Eastern Pacific and Western North America

[42] Measurements of particle properties obtained during ITCT 2K2 in westerly flow conditions show a complex and dynamic aerosol affected by a variety of sources and chemical and physical processes during transport. Measurements of particle and trace gas characteristics at the surface site at Trinidad Head during periods of unambiguous transpacific flow indicate that the MBL aerosol was generally decoupled from that aloft. The particles at the coastal site were dominated by sea salt in the super micron (coarse) mode, and by sulfate, ammonium, nitrate, and organics in the submicron (fine) mode [Allan *et al.*, 2004]. The organics present in the particles appear to be highly oxidized, probably because of the gradual oxidation and condensation of organic precursor gases during long-term transport from transpacific sources. The lifetime of the sulfate, nitrate, organic,

and number concentration component of the marine fine aerosol has been estimated using variability-lifetime relationships with VOCs to be  $\sim 4$ –10 days, while the lifetime of the ammonium and sea-salt components is shorter because of larger oceanic sources and sinks [Millet *et al.*, 2004a]. There is some evidence for displacement of the MBL aerosol by air with free tropospheric aerosol characteristics, in particular, enhanced concentrations of Asian crustal material, during the first few days of operations at the Trinidad head site (R. A. VanCuren *et al.*, Continental aerosol dominance above the marine boundary layer in the eastern North Pacific: Continuous aerosol measurements from the 2002 Intercontinental Transport and Chemical Transformation (ITCT 2K2) experiment, submitted to *Journal of Geophysical Research*, 2004) (hereinafter referred to as VanCuren *et al.*, submitted manuscript, 2004). This free tropospheric influence is not unambiguously identified in the gas-phase data [Millet *et al.*, 2004a]. Episodes influenced by coastal North American sources were evident in most of the aerosol data sets from Trinidad Head despite the relatively remote coastal location; their influence emphasizes that short instrumental sampling times and careful data evaluation are necessary to exclude contamination by local and regional sources.

[43] Above the MBL, a diverse range of particle properties were observed over the eastern Pacific and western North America during westerly flow conditions. Elemental analysis of size-segregated aerosol samples collected at two high-altitude surface sites, Trinity and Lassen, show a dominance of crustal components with peak mass loadings in the coarse size range, from 2.5 to 5  $\mu\text{m}$  diameter (VanCuren *et al.*, submitted manuscript, 2004). Submicron S, Pb, Zn, and K were associated with the crustal material and are characteristic of the aged Eurasian continental aerosol [VanCuren, 2003]. Airborne observations of particle size distributions, bulk submicron ionic composition, and single particle composition show that particle chemical and physical properties above the boundary layer were highly inhomogeneous in space and time. The aerosol could be characterized as a background of mixed sulfate-organic particles present at quite low concentrations, on which were superimposed layers of aerosol originating from industrial, biomass-biofuel, and crustal sources [Brock *et al.*, 2004; Hudson *et al.*, 2004]. The layers associated with these sources were often discrete and decoupled. For example, on 5 May 2002, a single vertical profile showed the presence of three distinct layers between 4 and 8 km; the upper one from Asian biomass-biofuel combustion, the middle one from Asian industrial-urban-biofuel sources, and the lower one containing coarse crustal particles from an unknown source [Brock *et al.*, 2004]. Throughout the study, particles identified as biomass-biofuel combustion origin contributed a surprising 30–40% of the total particle number concentration detected by the PALMS single-particle mass spectrometer in the free troposphere [Hudson *et al.*, 2004]. These particles were distinct from recently formed biomass-biofuel particles by the presence of sulfur compounds, presumably deposited during aging of the particles over long transport times.

[44] Analyses of the transport of the aerosol layers [Cooper *et al.*, 2004b; Brock *et al.*, 2004] are generally consistent with the findings from PEACE- B, TRACE-P, and other studies [Oshima *et al.*, 2004; Miyazaki *et al.*, 2003; Moore *et al.*, 2003; Jacob *et al.*, 2003; Crutzen and Lawrence, 2000] namely, that prefrontal lifting in WCBs and through frontal and postfrontal convection are the primary mechanisms for lifting polluted air from the Asian PBL into the free troposphere, where it may be transported across the Pacific. The importance of cloud processing of the polluted air is evident in the data from 17 May 2002. In this case, the insoluble or partially soluble gases  $\text{SO}_2$  and PAN were transported upward in the WCB of a Pacific wave cyclone, while existing aerosol particles and soluble gases were scavenged and removed by precipitation. In the ensuing several-day transport time in the free troposphere, thermal decomposition and photochemical conversion of the gases led to the formation of an aerosol layer rich in sulfuric acid particles and in gas-phase nitric acid [Brock *et al.*, 2004; Nowak *et al.*, 2004].

[45] Within the PBL over North America, local sources quickly dominated the characteristics of the Pacific air transported eastward over the continent. Over southern California, local and regional  $\text{NO}_x$  and ammonia sources produced rapid conversion of gas-phase nitric acid to the particle phase [Neuman *et al.*, 2003]. The spatial and vertical distribution of these ammonium nitrate particles is often governed by the source locations and by the atmospheric temperature profile. Local and regional biomass combustion sources can produce concentrated and dilute plumes with aerosol characteristics dominated by combustion-generated particles [Hudson *et al.*, 2004]. Thus within the continental PBL, local and regional sources dominate over long-range transport from transpacific sources. However, within the free troposphere, layers of particles of Eurasian origin remain and may affect midtropospheric cloud and chemical processes. Frontal activity and convection will add a North American component to the free tropospheric aerosol during further eastward transport.

#### 4. Conclusions

[46] The ITCT 2K2 and PEACE data sets comprise a remarkably rich data set for investigating the outflow from the emission regions on the Asian continent, their photochemical processing during transport across the Pacific, and their properties and impact upon arrival over North America. The results presented in this special section of JGR represent only the initial analysis; the data set will be available to the atmospheric chemistry community for further analysis in the coming years.

#### Appendix A: Comparison of Aircraft- and Sonde-Measured $\text{O}_3$ Profiles

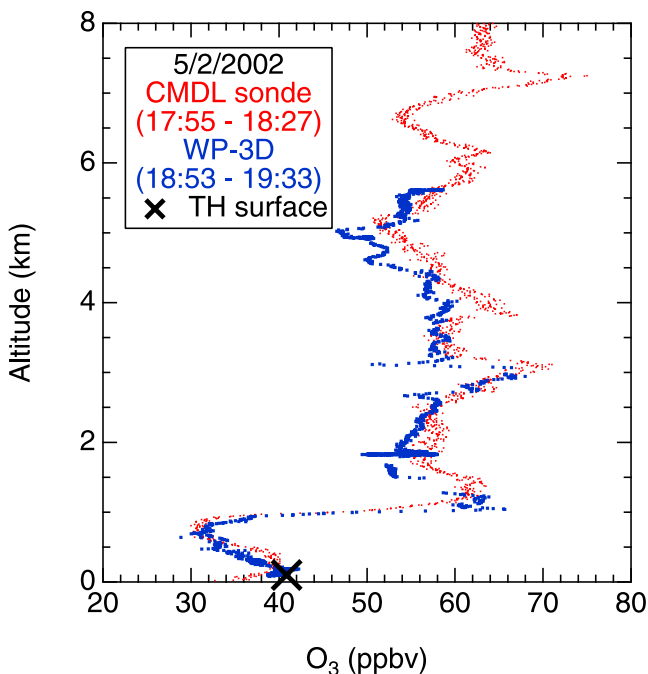
[47] During the ITCT 2K2 study the NOAA CMDL Laboratory launched daily  $\text{O}_3$  sondes from their site at Trinidad Head, California (see Figure 1). On six flights the NOAA WP-3D aircraft also measured  $\text{O}_3$  during vertical profiles flown in the vicinity of Trinidad Head.

Figure A1 shows the measured profiles for the aircraft flight most nearly coincident in time and location with a sonde launch. In general there is excellent agreement in magnitude and structure between the two profiles; the few ppbv differences can be attributed to differences in time and/or location of the profiles. The other 5 profiles showed larger differences, but they were also further apart in time ( $\leq 5$  hours) and/or location ( $\leq 150$  km). For five of the six flights the aircraft and the Trinidad Head ground site were in similar air masses at the lowest flight level of the aircraft. Excellent agreement was found between the aircraft and ground  $O_3$  instruments.

[48] To compare the data from vertical profiles from all six flights,  $O_3$  was averaged over 0.25 km altitude increments for both profiles on each day. These data were averaged for each 0.25 km increment for only those days when data were available from both measurements for that increment on that day. This procedure is deemed to give the most closely comparable data sets for the two techniques. Figure A2 shows the resulting comparison. The data scatter about the 1:1 line, and a linear regression with the intercept forced to zero (equivalent to assuming no offset in either technique) gives a slope statistically equivalent to unity.

[49] From these comparisons we conclude that the measurement of  $O_3$  at the surface site, from the NOAA WP-3D aircraft, and from the CMDL sondes, from the surface to the midtroposphere are consistent with each other, with no relative errors larger than 2 to 3 percent or offsets larger than 2 ppbv.

[50] Chen et al. (submitted manuscript, 2004) reached similar conclusions when they compared  $O_3$  sonde data from three Japanese stations with aircraft data collected during the PEACE and TRACE-P studies at the same



**Figure A1.**  $O_3$  profiles measured by  $O_3$  sonde and WP-3D aircraft. Here the cross indicates  $O_3$  measured at the Trinidad Head surface site at the time of the closest approach of the aircraft.

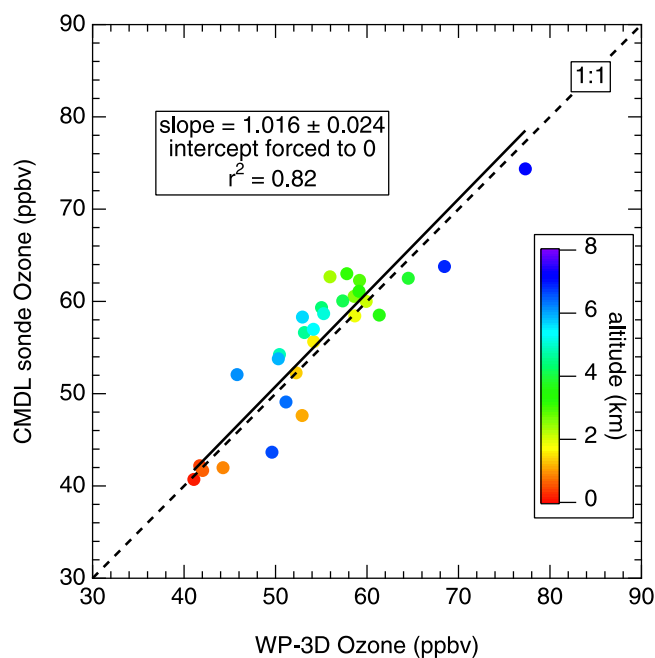


**Figure A2.** Comparison of average sonde and aircraft  $O_3$  data color-coded according to altitude for six vertical profiles flown over Trinidad Head during ITCT 2K2. The 95% confidence limit is given for the slope derived from a linear regression fit (solid line) with the intercept forced to zero.

latitude. Good agreement was found between these data, and these workers concluded that both measurements are representative of the atmosphere, and that they could use the data from both techniques in their analysis.

[51] **Acknowledgments.** The Climate and Global Change Program of the National Oceanic and Atmospheric Administration (NOAA) supported the ITCT 2K2 aircraft measurements. The Earth Observation Research and Application Center (EORC) of JAXA supported the PEACE aircraft measurements. The ITCT 2K2/PEACE campaigns were conducted under the framework of the International Global Atmospheric Chemistry (IGAC) project (<http://www.igac.noaa.gov/>).

## References

- Allan, J. D., J. L. Jimenez, P. I. Williams, M. R. Alfarra, K. N. Bower, J. T. Jayne, H. Coe, and D. R. Worsnop (2003), Quantitative sampling using an Aerodyne aerosol mass spectrometer: 1. Techniques of data interpretation and error analysis, *J. Geophys. Res.*, *108*(D3), 4090, doi:10.1029/2002JD002358.
- Allan, J., et al. (2004), Submicron aerosol composition at Trinidad Head, California, during ITCT 2K2: Its relationship with gas phase volatile organic carbon and assessment of instrument performance, *J. Geophys. Res.*, *109*, D23S24, doi:10.1029/2003JD004208.
- Andreae, M. O., H. Berresheim, T. W. Andreae, M. A. Kritz, T. S. Bates, and J. T. Merrill (1988), Vertical distribution of dimethylsulfide, sulfur dioxide, aerosol ions, and radon over the northeast Pacific Ocean, *J. Atmos. Chem.*, *6*, 149–173.
- Atlas, E. L., and B. A. Ridley (1996), The Mauna Loa Observatory Photochemistry Experiment: Introduction, *J. Geophys. Res.*, *101*, 14,531–14,541.
- Bench, G., P. G. Grant, D. Ueda, S. S. Cliff, K. D. Perry, and T. A. Cahill (2002), The use of STIM and PESA to respectively measure profiles of aerosol mass and hydrogen content across Mylar rotating drug impactor samples, *Aerosol Sci. Technol.*, *36*, 642–651.
- Bertschi, I. T., D. A. Jaffe, L. Jaeglé, H. U. Price, and J. B. Dennison (2004), PHOBEA/ITCT 2002 airborne observations of transpacific transport of ozone, CO, volatile organic compounds, and aerosols to the northeast Pacific: Impacts of Asian anthropogenic and Siberian boreal

- fire emissions, *J. Geophys. Res.*, *109*, D23S12, doi:10.1029/2003JD004328.
- Bey, I., D. J. Jacob, R. M. Yantosca, J. A. Logan, B. D. Field, A. M. Fiore, Q. Li, H. Y. Liu, L. J. Mickley, and M. G. Schultz (2001a), Global modeling of tropospheric chemistry with assimilated meteorology: Model description and evaluation, *J. Geophys. Res.*, *106*, 23,073–23,096.
- Bey, I., D. J. Jacob, J. A. Logan, and R. M. Yantosca (2001b), Asian chemical outflow to the Pacific: Origins, pathways and budgets, *J. Geophys. Res.*, *106*, 23,097–23,114.
- Brock, C. A., F. Schröder, B. Kärcher, A. Petzold, R. Busen, and M. Fiebig (2000), Ultrafine particle size distributions measured in aircraft exhaust plumes, *J. Geophys. Res.*, *105*(D21), 26,555–26,567.
- Brock, C. A., et al. (2003), Particle growth in urban and industrial plumes in Texas, *J. Geophys. Res.*, *108*(D3), 4111, doi:10.1029/2002JD002746.
- Brock, C. A., et al. (2004), Particle characteristics following cloud-modified transport from Asia to North America, *J. Geophys. Res.*, *109*, D23S26, doi:10.1029/2003JD004198.
- Cahill, T. A., and P. Wakabayashi (1993), Compositional analysis of size-segregated aerosol samples, in *Measurement Challenges in Atmospheric Chemistry*, edited by L. Newman, pp. 211–228, Am. Chem. Soc., Washington, D. C.
- Chan, C. Y., et al. (2004), Vertical profile and origin of wintertime tropospheric ozone over China during the PEACE-A period, *J. Geophys. Res.*, *109*, D23S06, doi:10.1029/2004JD004581.
- Coleman, J. J., A. L. Swanson, S. Meinard, B. C. Sive, D. R. Blake, and F. S. Rowland (2001), Description of the analysis of a wide range of volatile organic compounds in whole air samples collected during PEM-Tropics A&B, *Anal. Chem.*, *73*, 3723–3731.
- Cooper, O., et al. (2004a), On the life cycle of a stratospheric intrusion and its dispersion into polluted warm conveyor belts, *J. Geophys. Res.*, *109*, D23S09, doi:10.1029/2003JD004006.
- Cooper, O. R., et al. (2004b), A case study of transpacific warm conveyor belt transport: Influence of merging airstreams on trace gas import to North America, *J. Geophys. Res.*, *109*, D23S08, doi:10.1029/2003JD003624.
- Crutzen, P. J., and M. G. Lawrence (2000), The impact of precipitation scavenging on the transport of trace gases: A 3-dimensional model sensitivity study, *J. Atmos. Chem.*, *37*, 81–112.
- de Gouw, J. A., C. Warneke, T. Karl, G. Eerdeken, C. van der Veen, and R. Fall (2003), Sensitivity and specificity of atmospheric trace gas detection by proton-transfer-reaction mass spectrometry, *Int. J. Mass Spectrom. Ion Processes*, *223–224*, 365–382.
- de Gouw, J. A., et al. (2004), Chemical composition of air masses transported from Asia to the U.S. West Coast during ITCT 2K2: Fossil fuel combustion versus biomass-burning signatures, *J. Geophys. Res.*, *109*, D23S20, doi:10.1029/2003JD004202.
- Duce, R. A., C. K. Umri, B. J. Ray, J. M. Prospero, and J. T. Merrill (1980), Long-range atmospheric transport of soil dust from Asia to the tropical North Pacific: Temporal variability, *Science*, *209*, 1522–1524.
- Eisele, F. L., and D. J. Tanner (1993), Measurement of the gas phase concentration of H<sub>2</sub>SO<sub>4</sub> and methane sulfonic acid and estimates of H<sub>2</sub>SO<sub>4</sub> production and loss in the atmosphere, *J. Geophys. Res.*, *98*, 9001–9010.
- Forster, C., et al. (2004), Lagrangian transport model forecasts and a transport climatology for the Intercontinental Transport and Chemical Transformation 2002 (ITCT 2K2) measurement campaign, *J. Geophys. Res.*, *109*, D07S92, doi:10.1029/2003JD003589.
- Goldstein, A. H., D. B. Millet, M. McKay, L. Jaeglé, L. Horowitz, O. Cooper, R. Hudman, D. J. Jacob, S. Oltmans, and A. Clarke (2004), Impact of Asian emissions on observations at Trinidad Head, California, during ITCT 2K2, *J. Geophys. Res.*, *109*, D23S17, doi:10.1029/2003JD004406.
- Hess, P. G. (2001), Model and measurement analysis of springtime transport and chemistry in the Pacific basin, *J. Geophys. Res.*, *106*, 12,689–12,717.
- Hoell, J. M., Jr., D. L. Albritton, G. L. Gregory, R. J. McNeal, S. M. Beck, R. J. Bendura, and J. W. Drewry (1990), Operational overview of NASA GTE/CITE 2 airborne instrument intercomparisons: Nitrogen dioxide, nitric acid, and peroxyacetyl nitrate, *J. Geophys. Res.*, *95*, 10,047–10,054.
- Hoell, J. M., D. D. Davis, S. C. Liu, R. E. Newell, H. Akimoto, R. J. McNeal, and R. J. Bendura (1997), The Pacific Exploratory Mission-West Phase B: February–March, 1994, *J. Geophys. Res.*, *102*, 28,223–28,239.
- Holloway, J. S., R. O. Jakoubek, D. D. Parrish, C. Gerbig, A. Volz-Thomas, S. Schmitgen, A. Fried, B. Wert, B. Henry, and J. R. Drummond (2000), Airborne intercomparison of vacuum ultraviolet fluorescence and tunable diode laser absorption measurements of tropospheric carbon monoxide, *J. Geophys. Res.*, *105*, 24,251–24,261.
- Horowitz, L. W., et al. (2003), A global simulation of tropospheric ozone and related tracers: Description and evaluation of MOZART, version 2, *J. Geophys. Res.*, *108*(D24), 4784, doi:10.1029/2002JD002853.
- Hudman, R. C., et al. (2004), Ozone production in transpacific Asian pollution plumes and implications for ozone air quality in California, *J. Geophys. Res.*, *109*, D23S10, doi:10.1029/2004JD004974, in press.
- Hudson, P. K., D. M. Murphy, D. J. Cziczo, D. S. Thomson, J. A. de Gouw, C. Warneke, J. Holloway, H.-J. Jost, and G. Hübler (2004), Biomass-burning particle measurements: Characteristic composition and chemical processing, *J. Geophys. Res.*, *109*, D23S27, doi:10.1029/2003JD004398.
- Huebert, B. J., T. Bates, P. B. Russell, G. Shi, Y. J. Kim, K. Kawamura, G. Carmichael, and H. Nakajima (2003), An overview of ACE-Asia: Strategies for quantifying the relationships between Asian aerosols and their climatic impacts, *J. Geophys. Res.*, *108*(D23), 8633, doi:10.1029/2003JD003550.
- Jacob, D. J., J. H. Crawford, M. M. Kleb, V. S. Connors, R. J. Bendura, J. L. Raper, G. W. Sachse, J. C. Gille, L. Emmons, and C. L. Heald (2003), Transport and Chemical Evolution over the Pacific (TRACE-P) aircraft mission: Design, execution, and first results, *J. Geophys. Res.*, *108*(D20), 9000, doi:10.1029/2002JD003276.
- Jaeglé, L., D. A. Jaffe, H. U. Price, P. Weiss-Penzias, P. I. Palmer, M. J. Evans, D. J. Jacob, and I. Bey (2003), Sources and budgets for CO and O<sub>3</sub> in the northeast Pacific during the spring of 2001: Results from the PHOBEA-II experiment, *108*(D20), 8802, doi:10.1029/2002JD003121.
- Jaffe, D., T. Anderson, D. Covert, B. Trost, J. Danielson, W. Simpson, D. Blake, J. Harris, and D. Streets (2001), Observations of ozone and related species in the northeast Pacific during the PHOBEA campaigns: 1. Ground-based observations at Cheeka Peak, *J. Geophys. Res.*, *106*, 7449–7461.
- Jaffe, D., I. McKendry, T. Anderson, and H. Price (2003a), Six ‘new’ episodes of trans-Pacific transport of air pollutants, *Atmos. Environ.*, *37*, 391–404.
- Jaffe, D., H. Price, D. D. Parrish, A. Goldstein, and J. Harris (2003b), Increasing background ozone during spring on the west coast of North America, *Geophys. Res. Lett.*, *30*(12), 1613, doi:10.1029/2003GL017024.
- Jimenez, J. L., et al. (2003), Ambient aerosol sampling using the Aerodyne aerosol mass spectrometer, *J. Geophys. Res.*, *108*(D7), 8425, doi:10.1029/2001JD001213.
- Kita, K., et al. (2002), Photochemical production of ozone in the upper troposphere in association with cumulus convection over Indonesia, *J. Geophys. Res.*, *107*, 8400, doi:10.1029/2001JD000844. [printed 108(D3), 2003]
- Kondo, Y., S. Kawakami, M. Koike, D. W. Fahey, H. Nakajima, Y. Zhao, N. Toriyama, M. Kanada, G. W. Sachse, and G. L. Gregory (1997), Performance of an aircraft instrument for the measurement of NO<sub>x</sub>, *J. Geophys. Res.*, *102*, 28,663–28,671.
- Kondo, Y., M. Ko, M. Koike, S. Kawakami, and T. Ogawa (2002), Preface to Special Section on Biomass Burning and Lightning Experiment (BIBLE), *J. Geophys. Res.*, *107*, 8397, doi:10.1029/2002JD002401. [printed 108(D3), 2003]
- Kondo, Y., et al. (2004), Photochemistry of ozone over the western Pacific from winter to spring, *J. Geophys. Res.*, *109*, D23S02, doi:10.1029/2004JD004871.
- Kotchenruther, R. A., D. A. Jaffe, and L. Jaeglé (2001), Ozone photochemistry and the role of peroxyacetyl nitrate in the springtime northeastern Pacific troposphere: Results from the Photochemical Ozone Budget of the Eastern North Pacific Atmosphere (PHOBEA) campaign, *J. Geophys. Res.*, *106*, 28,731–28,742.
- Lawrence, M. G., et al. (2003), Global chemical weather forecasts for field campaign planning: Predictions and observations of large-scale features during MINOS, CONTRACE, and INDOEX, *Atmos. Chem. Phys.*, *3*, 267–289.
- Liang, Q., L. Jaeglé, D. A. Jaffe, P. Weiss-Penzias, A. Heckman, and J. A. Snow (2004), Long-range transport of Asian pollution to the northeast Pacific: Seasonal variations and transport pathways of carbon monoxide, *J. Geophys. Res.*, *109*, D23S07, doi:10.1029/2003JD004402.
- Liley, J. B., et al. (2002), Black carbon in aerosol during BIBLE B, *J. Geophys. Res.*, *107*, 8399, doi:10.1029/2001JD000845. [printed 108(D3), 2003]
- Machida, T., K. Kita, Y. Kondo, D. Blake, S. Kawakami, G. Inoue, and T. Ogawa (2002), Vertical and meridional distributions of the atmospheric CO<sub>2</sub> mixing ratio between northern midlatitudes and southern subtropics, *J. Geophys. Res.*, *107*, 8401, doi:10.1029/2001JD000910. [printed 108(D3), 2003]
- Millet, D. B., et al. (2004a), Volatile organic compound measurements at Trinidad Head, California, during ITCT 2K2: Analysis of sources, atmospheric composition, and aerosol residence times, *J. Geophys. Res.*, *109*, D23S16, doi:10.1029/2003JD004026.
- Millet, D. B., N. M. Donahue, S. N. Pandis, A. Polidori, C. O. Stanier, B. J. Turpin, and A. H. Goldstein (2004b), Atmospheric VOC measurements during the Pittsburgh Air Quality Study: Results, interpretation and quan-

- tification of primary and secondary contributions, *J. Geophys. Res.*, doi:10.1029/2004JD004601, in press.
- Miyazaki, Y., et al. (2003), Synoptic-scale transport of reactive nitrogen over the western Pacific in spring, *J. Geophys. Res.*, 108(D20), 8788, doi:10.1029/2002JD003248.
- Moore, K. G., II, A. D. Clarke, V. N. Kapustin, and S. G. Howell (2003), Long-range transport of continental plumes over the Pacific Basin: Aerosol physiochemistry and optical properties during PEM-Tropics A and B, *J. Geophys. Res.*, 108(D2), 8236, doi:10.1029/2001JD001451.
- Neuman, J. A., et al. (2002), Fast-response airborne in situ measurement of HNO<sub>3</sub> during the Texas Air Quality Study, *J. Geophys. Res.*, 107(D20), 4436, doi:10.1029/2001JD001437.
- Neuman, J. A., et al. (2003), Vertical gradients and spatial variability in ammonium nitrate formation and nitric acid depletion over California, *J. Geophys. Res.*, 108(D17), 4557, doi:10.1029/2003JD003616.
- Nowak, J. B., et al. (2004), Gas-phase chemical characteristics of Asian emission plumes observed during ITCT 2K2 over the eastern North Pacific Ocean, *J. Geophys. Res.*, 109, D23S19, doi:10.1029/2003JD004488.
- Orsini, D. A., Y. Ma, A. Sullivan, B. Sierau, K. Baumann, and R. J. Weber (2003), Refinements to the particle-into-liquid sampler (PILS) for ground and airborne measurements of water-soluble aerosol composition, *Atmos. Environ.*, 37, 1243–1259.
- Oshima, N., et al. (2004), Asian chemical outflow to the Pacific in late spring observed during the PEACE-B aircraft mission, *J. Geophys. Res.*, 109, D23S05, doi:10.1029/2004JD004976, in press.
- Parrish, D. D., C. J. Hahn, E. J. Williams, R. B. Norton, F. C. Fehsenfeld, H. B. Singh, J. D. Shetter, B. W. Gandrud, and B. A. Ridley (1992), Indications of photochemical histories of Pacific air masses from measurements of atmospheric trace species at Pt. Arena, California, *J. Geophys. Res.*, 97, 15,883–15,901.
- Parrish, D. D., et al. (2004a), Changes in the photochemical environment of the temperate North Pacific troposphere in response to increased Asian emissions, *J. Geophys. Res.*, 109, D23S18, doi:10.1029/2004JD004978, in press.
- Parrish, D. D., et al. (2004b), Fraction and composition of NO<sub>y</sub> transported in air masses lofted from the North American continental boundary layer, *J. Geophys. Res.*, 109, D09302, doi:10.1029/2003JD004226.
- Perry, K. D., T. A. Cahill, R. C. Schnell, and J. M. Harris (1999), Long-range transport of anthropogenic aerosols to the National Oceanic and Atmospheric Administration baseline station at Mauna Loa Observatory, Hawaii, *J. Geophys. Res.*, 104, 18,521–18,533.
- Price, H. U., D. A. Jaffe, P. V. Doskey, I. McKendry, and T. L. Anderson (2003), Vertical profiles of O<sub>3</sub>, aerosols, CO and NMHCs in the northeast Pacific during the TRACE-P and ACE-Asia experiments, *J. Geophys. Res.*, 108(D20), 8799, doi:10.1029/2002JD002930.
- Price, H. U., D. A. Jaffe, O. R. Cooper, and P. V. Doskey (2004), Photochemistry, ozone production, and dilution during long-range transport episodes from Eurasia to the northwest United States, *J. Geophys. Res.*, 109, D23S13, doi:10.1029/2003JD004400.
- Prospero, J. M. (1979), Mineral and sea-salt aerosol concentrations in various ocean regions, *J. Geophys. Res.*, 84, 725–731.
- Ridley, B. A., and E. Robinson (1992), The Mauna Loa Observatory Photochemistry Experiment, *J. Geophys. Res.*, 97, 10,285–10,290.
- Roberts, J. M., et al. (2004), Measurement of peroxyacetylic nitric anhydrides (PANs) during the ITCT 2K2 aircraft intensive experiment, *J. Geophys. Res.*, 109, D23S21, doi:10.1029/2004JD004960, in press.
- Ryerson, T. B., et al. (1998), Emissions lifetimes and ozone formation in power plant plumes, *J. Geophys. Res.*, 103, 22,569–22,583.
- Ryerson, T. B., L. G. Huey, K. Knapp, J. A. Neuman, D. D. Parrish, D. T. Sueper, and F. C. Fehsenfeld (1999), Design and initial characterization of an inlet for gas-phase NO<sub>y</sub> measurements from aircraft, *J. Geophys. Res.*, 104, 5483–5492.
- Ryerson, T. B., E. J. Williams, and F. C. Fehsenfeld (2000), An efficient photolysis system for fast-response NO<sub>2</sub> measurements, *J. Geophys. Res.*, 105, 26,447–26,461.
- Schauffler, S. M., E. L. Atlas, D. R. Blake, F. Flocke, R. A. Lueb, J. M. Lee-Taylor, V. Stroud, and W. Travnicek (1999), Distributions of brominated organic compounds in the troposphere and lower stratosphere, *J. Geophys. Res.*, 104, 21,513–21,535.
- Stohl, A., and D. J. Thomson (1999), A density correction for Lagrangian particle dispersion models, *Boundary Layer Meteorol.*, 90, 155–167.
- Stohl, A., M. Hittenberger, and G. Wotawa (1998), Validation of the Lagrangian particle dispersion model FLEXPART against large scale tracer experiment data, *Atmos. Environ.*, 24, 4245–4264.
- Streets, D. G., et al. (2003), An inventory of gaseous and primary aerosol emissions in Asia in the year 2000, *J. Geophys. Res.*, 108(D21), 8809, doi:10.1029/2002JD003093.
- Takegawa, N., et al. (2001), Airborne vacuum ultraviolet resonance fluorescence instrument for in situ measurement of CO, *J. Geophys. Res.*, 106, 24,237–24,244.
- Takegawa, N., et al. (2004), Removal of NO<sub>x</sub> and NO<sub>y</sub> in Asian outflow plumes: Aircraft measurements over the western Pacific in January 2002, *J. Geophys. Res.*, 109, D23S04, doi:10.1029/2004JD004866.
- Tang, Y., et al. (2004), Multiscale simulations of tropospheric chemistry in the eastern Pacific and on the U.S. West Coast during spring 2002, *J. Geophys. Res.*, 109, D23S11, doi:10.1029/2004JD004513.
- Thomson, D. S., M. E. Schein, and D. M. Murphy (2000), Particle analysis by laser mass spectrometry WB-57 instrument overview, *Aerosol Sci. Technol.*, 33, 153–169.
- VanCuren, R. A. (2003), Asian aerosols in North America: Extracting the chemical composition and mass concentration of the Asian continental aerosol plume from long term aerosol records in the western United States, *J. Geophys. Res.*, 108(D20), 4623, doi:10.1029/2003JD003459.
- Weber, R. J., D. Orsini, Y. Daun, Y.-N. Lee, P. Klotz, and F. Brechtel (2001), A particle-in-liquid collector for rapid measurement of aerosol chemical composition, *Aerosol Sci. Technol.*, 35, 718–727.
- Weiss-Penzias, P., D. A. Jaffe, A. McClintick, E. M. Prestbo, and M. S. Landis (2003), Gaseous elemental mercury in the marine boundary layer: Evidence for rapid removal in anthropogenic pollution, *Environ. Sci. Technol.*, 37(17), 3755–3763.
- Weiss-Penzias, P., D. A. Jaffe, L. Jaeglé, and Q. Liang (2004), Influence of long-range-transported pollution on the annual and diurnal cycles of carbon monoxide and ozone at Cheeka Peak Observatory, *J. Geophys. Res.*, 109, D23S14, doi:10.1029/2004JD004505.
- Whittlestone, S., and W. Zaborowski (1998), Baseline radon detectors for shipboard use: Development and deployment in the First Aerosol Characterization Experiment (ACE 1), *J. Geophys. Res.*, 103, 16,743–16,751.
- Wilson, J. C., B. G. Lafleur, H. Hilbert, W. R. Seebaugh, J. Fox, D. W. Gesler, C. A. Brock, B. J. Huebert, and J. Mullen (2004), Function and performance of a low turbulence inlet for sampling supermicron particles from aircraft platforms, *Aerosol Sci. Technol.*, 38, 790–802.

C. A. Brock, O. R. Cooper, F. C. Fehsenfeld, G. Hübler, D. D. Parrish, and M. Trainer, NOAA Aeronomy Laboratory, 325 Broadway R/AL4, Boulder, CO 80305, USA. (cbrock@al.noaa.gov; ocooper@al.noaa.gov; fcf@al.noaa.gov; gerd@al.noaa.gov; parrish@al.noaa.gov; trainer@al.noaa.gov)

D. A. Jaffe, Interdisciplinary Arts and Sciences, University of Washington-Bothell, 18115 Campus Way NE, Bothell, WA 98011, USA. (djaffe@u.washington.edu)

Y. Kondo, Research Center for Advanced Science and Technology, University of Tokyo, 4-6-1 Komaba, Meguro-ku, Tokyo 153-8904, Japan. (kondo@atmos.rcast.u-tokyo.ac.jp)

T. Ogawa, Earth Observation Research and Application Center, Japan Aerospace Exploration Agency, Harumi Island Triton Square Office Tower X 23F, 1-8-10 Harumi, Chuo-ku, Tokyo 104-6023, Japan. (ogawa.toshihiro@jaxa.jp)